

# CdSe quantum dots grown on ZnSe and Zn<sub>0.97</sub>Be<sub>0.03</sub>Se by molecular-beam epitaxy: Optical studies

Xuecong Zhou,<sup>a)</sup> Martin Muñoz, Shiping Guo, and Maria C. Tamargo<sup>b)</sup>  
*Department of Chemistry, The City College of CUNY, 138th St. and Convent Ave., New York, New York 10031*

Yi Gu, Igor L. Kuskovsky, and Gertrude F. Neumark  
*Department of Applied Physics and Applied Mathematics, Columbia University, New York, New York 10027*

(Received 27 October 2003; accepted 2 February 2004; published 8 June 2004)

We report detailed studies of the photoluminescence (PL) properties of CdSe quantum dots (QDs) grown on ZnSe and Zn<sub>0.97</sub>Be<sub>0.03</sub>Se by molecular-beam epitaxy. We performed steady-state and time-resolved PL measurements and observed that nonradiative processes dominate at room temperature (RT) in the CdSe/Zn<sub>0.97</sub>Be<sub>0.03</sub>Se QD structures while these nonradiative processes do not dominate in the CdSe/ZnSe QD structures up to RT. We developed a method to estimate the capped CdSe/Zn<sub>0.97</sub>Be<sub>0.03</sub>Se QD size and composition, based on PL and photoluminescence excitation as well as Raman scattering spectroscopy measurements. Assuming spherical QDs, we estimate the QD radii to be in the range of 2.5 nm to 4.0 nm with the Cd concentration in the range of 47%–54%. This size is smaller than the exciton Bohr radius, suggesting a nearly zero-dimensional character. We also performed contactless electroreflectance measurements on the CdSe/ZnSe QDs, and observed the transitions due to the QDs and the wetting layer. In this case, assuming lens-shaped QDs, we extracted the QD radius to be around 9.52 nm, the height about 3.24 nm. This size is larger than the exciton Bohr radius, indicating a quasi-two-dimensional character. Studies based on Raman scattering spectroscopy suggest that the Cd concentration is about 44% for this structure. The temperature dependences of the PL lifetimes are consistent with the results of the QD size and Cd concentration estimated by these two methods. © 2004 American Vacuum Society. [DOI: 10.1116/1.1690780]

## I. INTRODUCTION

Self-assembled quantum dots are of interest due to the low-dimensional physical phenomena they present as well as their potential for device applications. So far, most of the investigations have involved III–V systems, such as (In,Ga)As/GaAs,<sup>1</sup> InP/InGaP,<sup>2</sup> and GaSb/GaAs,<sup>3</sup> which are suited for the near-infrared range applications. Much less work has been done in II–VI systems, which are attractive for optoelectronic applications in the blue–green spectral regions.<sup>4</sup> In II–VI systems, CdSe/ZnSe is the most studied material so far partly due to its resemblance to the InAs/GaAs system in terms of band-gap difference and lattice mismatch.

We have recently reported growth of CdSe self-assembled quantum dots (SAQDs) on ZnSe and Zn<sub>0.97</sub>Be<sub>0.03</sub>Se by molecular-beam epitaxy (MBE).<sup>5</sup> The atomic force microscopy (AFM) and photoluminescence (PL) measurements show that the introduction of Be in the layer on which the CdSe quantum dots (QDs) are formed results in smaller size, higher density, and better uniformity of the QDs. In this article, we report detailed studies of the optical properties of these two types of QD structures. We observe that the PL intensities at room temperature (RT) for these two structures

are very different while they are comparable at low temperature. A time-resolved PL (TRPL) study reveals that nonradiative processes dominate at RT in the CdSe/Zn<sub>0.97</sub>Be<sub>0.03</sub>Se QD structure while these nonradiative processes do not dominate in the CdSe/ZnSe QD structure up to RT. We developed a method to estimate the capped CdSe/Zn<sub>0.97</sub>Be<sub>0.03</sub>Se QD size and Cd concentration, based on PL and photoluminescence excitation (PLE) as well as Raman scattering spectroscopy measurements. Assuming a spherical QD shape, the size and Cd concentration of the QDs were obtained. We also performed contactless electroreflectance (CER) measurements on the CdSe/ZnSe QDs, and observed transitions due to the QDs and the wetting layer. In this case, assuming lens-shaped QDs, the QD size was extracted. Studies based on Raman scattering spectroscopy suggest that the Cd concentration is about 44% for this structure. The temperature dependences of the PL lifetimes are consistent with the results of the QD size and Cd concentration estimated by these two methods.

## II. EXPERIMENTAL DETAILS

The samples were grown on epitaxially grown GaAs(001) substrate.<sup>5</sup> The sample structures consist of a 200 nm GaAs buffer layer, 30 periods of (2 nm GaAs/2 nm AlAs) short-period superlattice, a 30 nm GaAs layer, a 6 nm ZnSe buffer layer, a 94 nm Zn<sub>0.97</sub>Be<sub>0.03</sub>Se (or ZnSe) layer, above which, CdSe QDs formed by depositing 2.5 monolayers of CdSe, and a 100 nm Zn<sub>0.97</sub>Be<sub>0.03</sub>Se (or ZnSe) cap layer.

<sup>a)</sup>Also at Department of Physics and Astronomy, Hunter College of CUNY, New York, NY 10021; electronic mail: cong999@yahoo.com

<sup>b)</sup>Author to whom correspondence should be addressed; electronic mail: tamar@sci.cny.cuny.edu

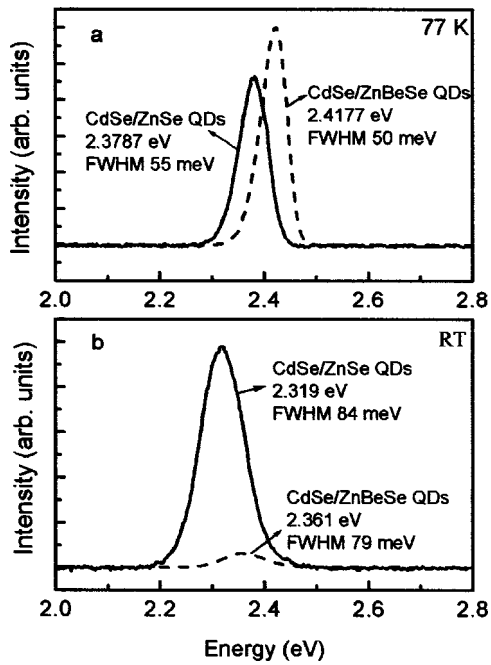


FIG. 1. Steady-state PL intensity profiles at 77 K (a) and RT (b) for CdSe QDs grown on ZnSe (solid line) and on  $Zn_{0.97}Be_{0.03}Se$  (dashed line).

Time-resolved PL measurements were carried out using the second harmonic of an amplified colliding pulse mode-locking (CPM) output (pulse width=100 fs, repetition rate=5 kHz) at a 305 nm wavelength. The spectrally integrated emission of the sample was obtained by using a streak camera with a time resolution of 10 fs. The temperature dependent measurements were performed in a liquid-nitrogen continuous flow cryostat with a temperature control unit.

For the steady-state PL measurement, a 325 nm line of the He–Cd laser was used as the excitation source. The PL was recorded with a 0.75 m monochromator, a thermoelectrically cooled GaAs photomultiplier tube, and a SR400 photon counter. For PLE measurements, a 300 W xenon lamp, coupled with a 0.25 m monochromator, was used.

Contactless electroreflectance measurement utilizes a condenserlike system<sup>6</sup> consisting of a front wire grid electrode with a second metal electrode separated from the first electrode by insulating spacers, which are  $\sim 0.1 \mu\text{m}$  larger than the sample dimension. The sample was placed between these two capacitor plates and the electromodulation was achieved by applying an ac voltage of 1.2 kV, 200 Hz across the electrodes.

### III. RESULTS AND DISCUSSION

The steady-state PL intensity profiles at 77 K and RT for the two samples investigated are shown in Figs. 1(a) and 1(b), respectively. At each temperature, the measurements were made under identical instrumental conditions so the relative intensities could be compared. The slightly higher peak position and narrower linewidth of the ZnBeSe-based sample are attributed to the smaller and more uniformly sized islands in this structure.<sup>5</sup> Interestingly, Figs. 1(a) and

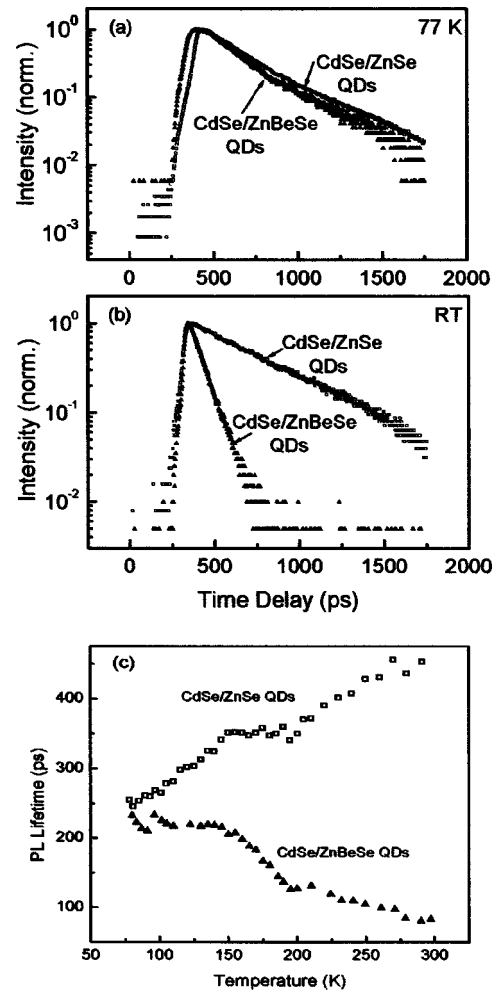


FIG. 2. TRPL at 77 K (a) and RT (b) for CdSe QDs grown on ZnSe (open squares) and on  $Zn_{0.97}Be_{0.03}Se$  (solid triangles). (c) Temperature dependences of PL decay time for CdSe QDs grown on ZnSe (open squares) and on  $Zn_{0.97}Be_{0.03}Se$  (solid triangles).

1(b) show that the steady-state PL intensity from the CdSe QDs on ZnSe measured at RT is much higher than that from CdSe QDs on  $Zn_{0.97}Be_{0.03}Se$  while the two have similar intensities at 77 K.

To better understand the PL intensity relationship at these two temperatures, we have performed TRPL measurements on both samples as a function of temperature, in the range of 77 K to RT. The PL decay profiles at 77 K and RT for the two samples are shown in Figs. 2(a) and 2(b). (A small kink observed at about 869 ps–951 ps is due to the streak camera error in this time region, and the slight downward bend at the end is due to background subtraction.) While at 77 K the two decay traces nearly overlap and have a comparable rate of decay, at RT the ZnBeSe-based QD sample exhibits a much faster PL decay rate than the ZnSe-based QD sample. In these measurements, QDs of all sizes contribute to the time decay. It has been previously shown<sup>7</sup> that the PL lifetime for different QDs depends on the QD size, thus measurements of an ensemble of QDs lead to a distribution of lifetimes. It is also known that decay at a single wavelength for these structures is a single exponential at most of the wavelengths.<sup>8</sup> Thus, our observed decay (based on spectrally integrated

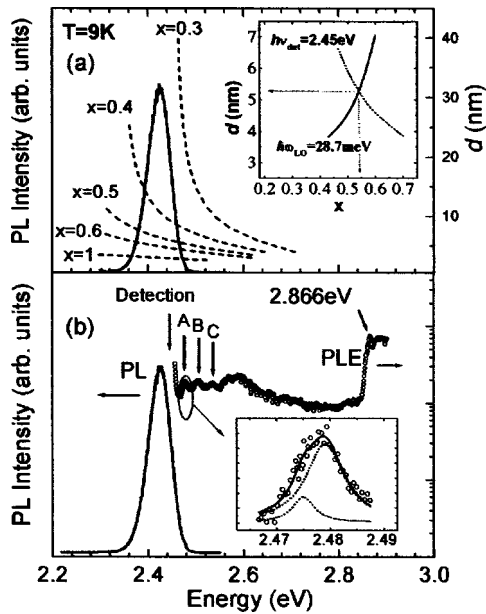


FIG. 3. (a) Calculated PL emission energies (dashed lines) for  $\text{Cd}_x\text{Zn}_{1-x}\text{Se}/\text{Zn}_{0.97}\text{Be}_{0.03}\text{Se}$  QDs as a function of  $x$  and  $d$ . The PL spectrum ( $T=9$  K) is also shown. The inset shows an example for estimation of  $x$  and  $d$ ; (b) The PL (solid line) and PLE spectra (open circles, plotted in a semilog scale) for the  $\text{CdSe}/\text{Zn}_{0.97}\text{Be}_{0.03}\text{Se}$  QD sample at  $T=9$  K. The detection energy and three equally spaced peaks (A, B, and C) are indicated by arrows. The inset is the magnification of the marked region in the PLE spectrum: Open circles represent the experimental data, and the solid line is the result of the fitting with two Lorentzians (dashed lines).

measurements of many QDs) is expected to be a sum of such exponentials weighed by a distribution function. It has been stated<sup>9</sup> that such a sum can be replaced by a stretched exponential function  $I(t) = I(0)\exp(-((t-t_0)/\tau)^\beta)$ , where  $\tau$  is the PL lifetime and  $\beta$  represents the broadening of the distribution function (or QD size distribution, in our case). Based on these considerations, we used the stretched exponential decay to fit the PL lifetimes. Thus, the PL lifetimes obtained here should be treated as average or representative PL lifetimes. Shown in Fig. 2(c) are the temperature dependences of the PL lifetimes obtained by this analysis. The temperature dependences of the PL lifetimes for the two samples are strikingly different. The PL lifetime for CdSe QDs grown on ZnSe is about 255 ps at 77 K and increases steadily all the way to about 453 ps at RT. For CdSe QDs grown on  $\text{Zn}_{0.97}\text{Be}_{0.03}\text{Se}$ , the PL lifetime is about 232 ps at 77 K and goes down to about 83 ps at RT. A faster PL decay rate with increased temperatures, as observed for the ZnBeSe-based samples, has also been observed and reported for other low-dimensional systems.<sup>10,11</sup> This behavior was attributed to unspecified nonradiative phenomena that become dominant at high temperatures. However, we do not observe such dominant nonradiative processes even at RT in the sample of the CdSe QDs grown on ZnSe. The absence of dominant nonradiative processes at RT has important implications for light-emitting devices in which RT operation is desired.

The PL ( $T=9$  K) from  $\text{CdSe}/\text{Zn}_{0.97}\text{Be}_{0.03}\text{Se}$  (solid line) QDs is shown in Fig. 3(a). Such a broad PL is usually observed in  $\text{Cd}_x\text{Zn}_{1-x}\text{Se}/\text{ZnSe}$  QD structures and attributed to

excitons localized in QDs with different concentrations ( $x$ ) and/or sizes (diameter  $d$ , assuming a spherical QD).<sup>12</sup> To estimate the  $x$  and the  $d$  of the QDs that are responsible for such a PL emission, as an initial step, we calculate the PL transition energy as a function of these two parameters. Details of the calculation of the PL energy as a function of  $x$  and  $d$  could be found in Ref. 13. We plot the results, shown in Fig. 3(a) (dashed lines), as the PL emission energy versus QD diameter (right-hand side axis) for a given Cd concentration. Comparing these calculated curves to the experimentally observed PL, such a plot shows conclusively that only QDs with Cd concentration greater than 30% can contribute to the observed PL emission. To determine both the  $x$  and the  $d$  of the QDs that contribute to the PL at a given wavelength, two independent measurements are necessary. This is illustrated in the inset of Fig. 3(a). The second measurement that we used is the longitudinal optical (LO) phonon energy obtained at a given wavelength using PLE. The PLE spectra on  $\text{CdSe}/\text{Zn}_{0.97}\text{Be}_{0.03}\text{Se}$  QD structure ( $T=9$  K) with detection energy ( $\hbar\nu_{\text{det}}$ ) at 2.45 eV (indicated by the arrow) is plotted in Fig. 3(b) along with the PL. The PLE spectrum consists of (1) a sharp strong peak at about 2.866 eV, which corresponds to the free exciton energy in  $\text{Zn}_{0.97}\text{Be}_{0.03}\text{Se}$ ,<sup>14</sup> (2) a rather broadband feature below this peak, which is presumably due to excitation via the CdZnSe wetting layer, and (3) three equally spaced peaks (indicated by A, B, and C) adjacent to the detection energy. The energy separation between these peaks as well as between the detection energy and peak A is around 28 meV, which is in the range of  $\text{Cd}_x\text{Zn}_{1-x}\text{Se}$  alloy LO phonon energy ( $\hbar\omega_{\text{LO}}$ ). A more careful investigation [see the inset of Fig. 3(b)] of peak A reveals that it can be fitted well with two Lorentzians, whose energy separations from  $\hbar\nu_{\text{det}}$  is  $\sim 28.7$  meV (peak 1) and 24.7 meV (peak 2), both attributed to LO phonons from  $\text{Cd}_x\text{Zn}_{1-x}\text{Se}$  QDs with a given concentration  $x$  and to surface phonons, respectively. We then proceed to quantitatively estimate  $\hbar\omega_{\text{LO}}(x, d)$  for  $\text{Cd}_x\text{Zn}_{1-x}\text{Se}$  QDs as a function of  $x$  (strain included) and  $d$  using the method developed in Refs. 15 and 16, assuming the linear interpolation between the CdSe and ZnSe values. Combining the calculations of the PL transition energies and LO phonon energies as well as the LO phonon energy data obtained from PLE, we are now able to estimate the Cd concentration and size of the QDs emitting at a given wavelength [shown in the inset of Fig. 3(a) is an example at a detection energy  $\hbar\nu_{\text{det}}=2.45$  eV] and obtain that the QD diameter ranges from 5.1 nm to 8.0 nm with a Cd concentration between 47% and 54%.<sup>13</sup> It is interesting that the radii estimated for the QDs (2.5 nm–4.0 nm) are smaller than the exciton Bohr radius in CdSe ( $\sim 5.4$  nm),<sup>17</sup> suggesting a nearly zero-dimensional character.

This analysis has the limitation that the assumed geometry of the QD (spherical) is not realistic. A more realistic picture might be to consider the dots to be a spherical “cap” (lens shape). The above analysis also requires that we observe the LO-phonon lines in the PLE spectrum, which was not possible in the CdSe/ZnSe QD structure. The absence of these



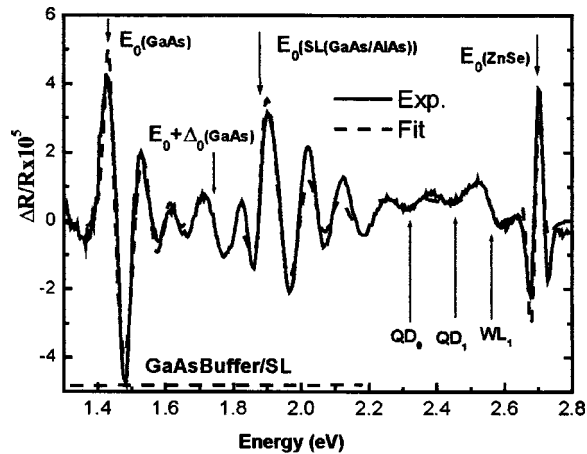


FIG. 4. CER spectrum at RT for the CdSe/ZnSe QD structure, where the solid line represents the experimental data and the dashed line is the fit. The transitions are indicated by the arrows.

lines suggests<sup>18</sup> that the “QDs” in this structure are larger than those in the CdSe/Zn<sub>0.97</sub>Be<sub>0.03</sub>Se structure (the Cd concentrations are similar for both structures, as will be shown below). Thus, a different analysis was needed for the CdSe/ZnSe QDs structure.

Shown in Fig. 4 is the measured RT CER spectrum (solid line) and the fitting (dashed line) for CdSe/ZnSe QD structure. The energies corresponding to the observed transitions are indicated by arrows and were obtained using the following fit scheme. The transitions originating in the superlattice buffer region (<2.2 eV) present a series of Franz–Keldysh oscillations, and were fit using Lorentzian broadened electro-optical functions.<sup>19</sup> The transitions originating from the QDs, wetting layer, and barrier (>2.2 eV) were fit using the first derivative of a Gaussian line shape<sup>19</sup> due to their bound origin. In order to identify the transitions originating from the QDs, the shape of the quantum lens in real space has been modeled by a spherical cap of height  $h$  and circular cross section with radius  $r$ . It is possible to show that for a QD with lens-shape geometry, the energy of the transitions depend on the ratio  $h/r$ , the energy levels  $N_e$  and  $N_h$ , and the angular momentum numbers  $M_e$  and  $M_h$ , for the electron and hole, respectively.<sup>20</sup> According to the allowed optical selection rule,  $N_e = N_h$ ,  $M_e = M_h$ , the features observed in the CdSe QD spectral region correspond to the transitions  $|N, M\rangle_e \rightarrow |N, M\rangle_h$ . Assuming that the effective ratio  $h/r$  ( $\sim 0.34$  obtained by AFM measurement) minimizes the surface energy in this system and, therefore, is the most favorable ratio for QDs formation, and assuming pure CdSe QDs, using the effective masses taken from Ref. 21, we determined that the dimensions of the capped CdSe QDs corresponding to these QD<sub>0</sub> and QD<sub>1</sub> transitions are  $h = 3.24$  nm and  $r = 9.52$  nm.<sup>22</sup> The QD size should be larger if intermixing is considered. This result shows that the radius of the QDs in this structure is larger than the exciton Bohr radius, suggesting a quasi-two-dimensional character, consistent with the absence of the LO-phonon lines in PLE.

The above analysis estimates the QD size only at a given

Cd concentration. In order to obtain information about the Cd concentration of the CdSe/ZnSe QDs, another measurement is necessary. From the preliminary studies using polarized Raman scattering spectroscopy with the excitation of 514.5 nm, we obtained the LO-phonon energy of the CdSe/ZnSe QDs. Following a similar procedure to that used above for the CdSe/Zn<sub>0.97</sub>Be<sub>0.03</sub>Se QDs, calculations based on the quantum disk model suggest that the Cd concentration is about 44%.<sup>23</sup>

Based on the results shown above, we propose that the presence of Be in the barrier layer makes the QD size smaller but does not affect the intermixing in the QDs. The CdSe/Zn<sub>0.97</sub>Be<sub>0.03</sub>Se QDs are very small, exhibiting nearly zero-dimensional quantum confinement, consistent with the temperature dependent TRPL results where the PL lifetime is about 232 ps at 77 K and remains nearly constant up to 150 K. Due to the small size of the QDs (low ionization energy), the PL lifetime goes down to about 83 ps at RT where the nonradiative processes dominate. In the case of CdSe/ZnSe QDs, the QD size is large, showing a quasi-two-dimensional behavior, consistent with the temperature dependent TRPL results where the PL lifetime is about 255 ps at 77 K and increases with increasing temperature. Due to the large size of the QDs (very high ionization energy), the PL lifetime increases steadily all the way to about 453 ps at RT without the effect of the dominant nonradiative processes.

In summary, we report detailed studies of the optical properties of CdSe QDs grown on ZnSe and Zn<sub>0.97</sub>Be<sub>0.03</sub>Se by MBE. We performed TRPL measurements and obtained the PL lifetimes for these two structures. We also estimated the QD size and Cd concentration due to the intermixing using different methods. The results of the PL lifetimes are consistent with the estimates of the QD size and Cd concentration obtained.

## ACKNOWLEDGMENTS

This work was supported by the National Science Foundation Grant No. ECS0217646. Partial support was also obtained from the New York Science and Technology Foundation through its CUNY Center for Advanced Technology on Photonic Materials and Applications and from the Center for Analysis of Structures and Interfaces.

<sup>1</sup>A. Madhukar, Q. Xie, P. Chen, and A. Konkar, *Appl. Phys. Lett.* **64**, 2727 (1994).

<sup>2</sup>A. Kurtenbach, E. Eberl, and T. Shitara, *Appl. Phys. Lett.* **66**, 361 (1995).

<sup>3</sup>F. Hatami, N. N. Ledentsov, M. Grundmann, J. Böhrer, F. Heinrichsdorff, M. Beer, D. Bimberg, S. S. Ruvimov, P. Werner, U. Gosele, J. Heydenreich, U. Richter, S. V. Ivanov, B. Y. Meltser, P. S. Kop'ev, and Z. Alferov, *Appl. Phys. Lett.* **67**, 656 (1995).

<sup>4</sup>S. H. Xin, P. D. Wang, A. Yin, C. Kim, M. Dobrowolska, J. L. Merz, and J. K. Furdyna, *Appl. Phys. Lett.* **69**, 3884 (1996).

<sup>5</sup>S. P. Guo, X. Zhou, O. Maksimov, M. C. Tamargo, C. Chi, A. Couzis, C. Maldarelli, I. L. Kuskovsky, and G. F. Neumark, *J. Vac. Sci. Technol. B* **19**, 1635 (2001).

<sup>6</sup>F. H. Pollak, in *Group III Nitride Semiconductor Compounds*, edited by B. Gil (Clarendon, Oxford, 1998), p. 158.

<sup>7</sup>Z. H. Zheng, K. Okamoto, H. C. Ko, Y. Kawakami, and S. Fujita, *Appl. Phys. Lett.* **78**, 297 (2001).

<sup>8</sup>B. P. Zhang, K. Wakatsuki, D. D. Manh, and Y. Segawa, *J. Appl. Phys.* **88**, 4916 (2000).

<sup>9</sup>I. Svara, S. W. Martin, and F. Borsa, *Phys. Rev. B* **61**, 228 (2000).

- <sup>10</sup>J. S. Massa, G. S. Buller, A. C. Walker, G. Horsburgh, J. T. Mullins, K. A. Prior, and B. C. Cavenett, *Appl. Phys. Lett.* **66**, 1346 (1995).
- <sup>11</sup>L. Marsal, L. Besombes, F. Tinjod, K. Kheng, A. Wasieleski, B. Gilles, J.-L. Rouvière, and H. Mariette, *J. Appl. Phys.* **91**, 4936 (2002).
- <sup>12</sup>J. K. Furdyna, S. Lee, A.-L. Barabási, and J. L. Merz, in *II–VI Semiconductor Materials and their Applications*, edited by M. C. Tamargo (Taylor and Francis, New York, 2002).
- <sup>13</sup>Y. Gu, Igor L. Kuskovsky, J. Fung, R. Robinson, I. P. Herman, G. F. Neumark, X. Zhou, S. P. Guo, and M. C. Tamargo, *Appl. Phys. Lett.* **83**, 3779 (2003).
- <sup>14</sup>C. Chauvet, E. Tournié, and J.-P. Faurie, *Phys. Rev. B* **61**, 5332 (2000).
- <sup>15</sup>E. Roca, *Phys. Rev. B* **49**, 13704 (1994).
- <sup>16</sup>M. P. Chamberlain, C. Trallero-Giner, and M. Cardona, *Phys. Rev. B* **51**, 1680 (1995).
- <sup>17</sup>H. Fu, L.-W. Wang, and A. Zunger, *Phys. Rev. B* **59**, 5568 (1999).
- <sup>18</sup>D. V. Melnikov and W. B. Fowler, *Phys. Rev. B* **64**, 245320 (2001).
- <sup>19</sup>F. H. Pollak and H. Shen, *Mater. Sci. Eng., R.* **10**, 275 (1993).
- <sup>20</sup>A. H. Rodríguez, C. Trallero-Giner, S. E. Ulloa, and J. Marín-Antuña, *Phys. Rev. B* **63**, 125319 (2001); A. H. Rodríguez, C. R. Handy, and C. Trallero-Giner, *J. Phys: Condens. Matter* **15**, 8465 (2003).
- <sup>21</sup>R. E. Nahory, M. J. S. P. Brasil, and M. C. Tamargo, in *Semiconductor Interfaces and Microstructures*, edited by Z. Feng (World Scientific, Singapore, 1992), p. 238.
- <sup>22</sup>M. Muñoz, S. Guo, X. Zhou, M. C. Tamargo, Y. S. Huang, C. Trallero-Giner, and A. H. Rodríguez, *Appl. Phys. Lett.* **83**, 4399 (2003).
- <sup>23</sup>Y. Gu, I. L. Kuskovsky, J. Fung, R. Robinson, I. P. Herman, G. F. Neumark, X. Zhou, S. P. Guo, and M. C. Tamargo (unpublished).